



# Study of anomalous wave propagation and reflection in semi-infinite elastic metamaterials



R. Zhu<sup>a,1,2</sup>, X.N. Liu<sup>b,1</sup>, G.L. Huang<sup>a,\*</sup>

<sup>a</sup> Department of Systems Engineering, University of Arkansas at Little Rock, Little Rock, AR 72204, USA

<sup>b</sup> School of Aerospace Engineering, Beijing Institute of Technology, Beijing 100081, People's Republic of China

## HIGHLIGHTS

- We study wave propagation in semi-infinite elastic metamaterials.
- A complete wave mode conversion is numerically demonstrated.
- Negative refraction of elastic waves is captured by the generalized Snell's law.
- Effects of negative properties on wave propagation are illustrated.

## ARTICLE INFO

### Article history:

Received 15 June 2014

Received in revised form 29 December 2014

Accepted 31 December 2014

Available online 20 January 2015

### Keywords:

Wave propagation

Elastic metamaterial

Generalized Snell's law

Negative material properties

## ABSTRACT

Elastic metamaterials have been investigated to achieve negative effective properties, which cannot be found in the conventional elastic medium. In this paper, plane wave propagation and reflection in semi-infinite elastic metamaterials with doubly or triply negative material properties are studied analytically and numerically. The unique negative refractions for the longitudinal (P) wave and transverse (S) wave are captured by the proposed generalized Snell's law. Attention is paid to quantitative characterization of the effects of different negative property combinations on the anomalous wave propagation. The effects of different angles of incidence are also investigated for both double-negative and triple-negative transmitted media and some unusual wave propagation phenomena such as complete wave mode conversion are numerically demonstrated. This study can serve as the theoretical foundation for engineering and designing general metamaterial-based elastic wave devices.

© 2015 Elsevier B.V. All rights reserved.

## 1. Introduction

Metamaterials have become a subject of great interest because of their abilities to achieve negative effective material properties unlike those of any conventional materials by introducing subwavelength resonators into their building blocks [1–7]. Double-negative electromagnetic (EM) metamaterials denote those artificial structures in which both the dielectric constant and magnetic permeability are simultaneously negative within a certain frequency regime [1,2]. Recently, the acoustic metamaterial, an analogue of the EM metamaterial, has also received considerable attention due to its exotic

\* Correspondence to: Department of Mechanical and Aerospace Engineering, University of Missouri-Columbia, MO 65211, USA. Tel.: +1 501 683 7522; fax: +1 501 569 8698.

E-mail address: [glhuang@ualr.edu](mailto:glhuang@ualr.edu) (G.L. Huang).

<sup>1</sup> These authors contributed equally to this work.

<sup>2</sup> Present address: Department of Mechanical and Aerospace Engineering, North Carolina State University, Raleigh, NC 27695-7910, USA.

acoustic properties such as negative effective mass density and/or bulk modulus. These metamaterials are compelling in view of the possibility of using negative refraction to design flat superlenses that can beat the diffraction limit [3].

Different from the acoustic metamaterial, the elastic metamaterial is a structured composite with a solid host matrix, which can support both longitudinal and transverse waves. Because of the vector characteristics of elastic waves and the possible coupling between the longitudinal and transverse wave modes, richer wave propagation phenomena are expected in the elastic metamaterial. Three independent effective parameters are required to completely characterize the solid material: effective bulk modulus, effective shear modulus, and effective mass density. The negative values of each single effective parameter and their various combinations can lead to eight kinds of elastic materials, which is twice as many as those in the EM and acoustic cases. Different microstructures were proposed to achieve the negative effective mass density and modulus, respectively. The negative effective mass density was experimentally demonstrated through a locally resonant structure by embedding soft silicon rubber coated lead spheres into an epoxy matrix medium [4]. The negative modulus, on the other hand, was demonstrated through an array of subwavelength Helmholtz resonators [5]. Extended theoretical studies on negative effective material properties were conducted by Milton and Willis [6] through a mass–spring model and by Movchan and Slepyan [7]. Dipolar and monopolar local resonances are regarded as the interior wave mechanisms for the negative mass density and the negative bulk modulus of the elastic metamaterial, respectively [8,9]. Liu et al. [10] first proposed a chiral elastic metamaterial with simultaneously translational and rotational resonances to achieve negative mass density and negative bulk modulus in certain frequency ranges. Negative refraction of a double-negative elastic metamaterial with single-phase chiral microstructure was experimentally demonstrated [11]. A metamaterial comprised of a fluid–solid multi-phase composite to enhance the quadrupolar resonance was suggested to possess simultaneously negative mass density and negative shear modulus and therefore, achieve negative refraction over a large frequency region [12]. Discrete structural interfaces with negative properties were also proposed to achieve negative refraction and flat lens focusing of elastic waves [13]. Most recently, Antonakakis et al. [14] presented high frequency asymptotic analysis for elastic waves leading to dynamic effective properties. Various novel concepts and engineering applications of elastic metamaterials have been successfully demonstrated such as seismic wave filters, sound and vibration isolators, elastic waveguides and energy harvesters [15–21].

Elastic wave propagation in solid media is an old subject and fruitful results and techniques can be found in many classic wave propagation books [22,23]. However, the introduction of elastic metamaterials broadens the horizon of this subject. In order to study the anomalous wave behavior and explore related engineering applications of elastic metamaterials, there is a great desire to investigate the wave propagation and reflection behavior in semi-infinite elastic media with various negative material properties. In this paper, plane wave propagation and reflection involving semi-infinite elastic media with doubly or triply negative properties are studied analytically and numerically. Various combinations of positive and negative material properties in transmitted elastic media are considered for different angles of incidence. Anomalous wave phenomena, such as negative refractions and complete wave mode conversion between the longitudinal and transverse waves, are investigated. The study can serve as the theoretical foundation for engineering and designing general metamaterial-based elastic wave devices. The paper is arranged in four sections including this introduction: in Section 2, the plane wave propagation involving the semi-infinite elastic metamaterial with negative material properties and standard positive elastic medium is analytically formulated; in Section 3, numerical results and related discussions for the anomalous wave reflection and refraction are presented. The effects of different negative property combinations on the anomalous wave propagation is quantitatively investigated for various angles of incidence. Finally, conclusions are presented in Section 4.

## 2. Plane wave propagation and reflection in the elastic media with negative material properties

A linear isotropic elastic medium can be characterized by Lamé constants  $\lambda$ ,  $\mu$  and the mass density  $\rho$ . In two dimensional (2D) plane strain problems, the P wave modulus is  $E_M = \lambda + 2\mu$  [24] and  $\mu$  is the shear wave modulus. Therefore, wave dispersion relations of the P and S waves can be determined by:

$$\mathbf{k} \cdot \mathbf{k} = \begin{cases} \frac{\omega^2 \rho}{E_M}, & \text{for the P wave} \\ \frac{\omega^2 \rho}{\mu}, & \text{for the S wave} \end{cases} \quad (1)$$

where  $\mathbf{k}$  is the wave vector and  $\omega$  is the angular frequency. Based on the definition, the magnitude of wave vector  $\mathbf{k}$  should be an imaginary number if the elastic medium possesses positive modulus and negative mass density, which implies that the elastic wave is prohibited in such medium. However, the magnitude of wave vector  $\mathbf{k}$  can be a positive real number when both the modulus and density are negative, which means that the elastic waves can propagate in the medium with double-negative or triple-negative material properties. The energy flow in the elastic medium can be described by the Poynting vector  $\mathbf{P}$  as:

$$\mathbf{P} = -\mathbf{v}^* \cdot \boldsymbol{\sigma}, \quad (2)$$

where  $\boldsymbol{\sigma}$  is the stress field tensor,  $\mathbf{v}$  is the particle velocity vector and the asterisk denotes a complex conjugate. Without loss of generality, let us consider only the P wave propagation [25]:

$$\mathbf{k} \cdot \mathbf{P} = \frac{1}{2} \omega \rho |\mathbf{v}_p|^2 \quad (3)$$

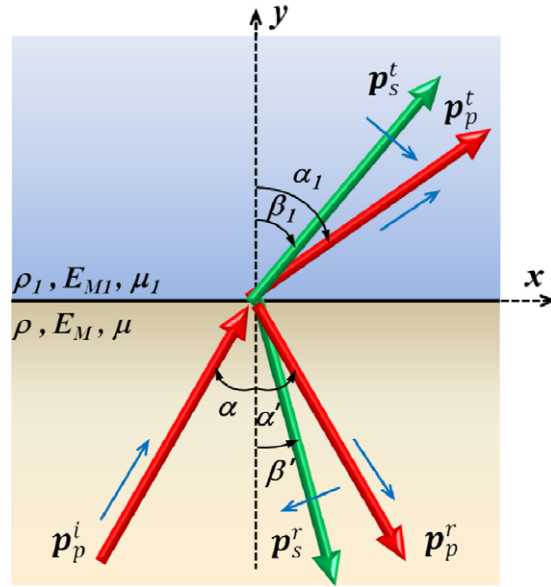


Fig. 1. The P wave incident at the interface between two elastic media.

Table 1

Transmitted media with various combinations of material properties and the corresponding refraction angles and amplitudes of the transmission coefficients of the refracted P and S waves.

Catalog of the transmitted medium	Material properties of the transmitted medium			Refraction angles		Amplitudes of the transmission coefficients	
	$\rho_1$ (kg/m <sup>3</sup> )	$E_{M1}$ (GPa)	$\mu_1$ (GPa)	P ( $\alpha_1$ )	S ( $\beta_1$ )	P ( $ T_p^t $ )	S ( $ T_s^t $ )
All-positive	2700	100	59	42.2°	31.0°	0.89	0.34
Single-negative	-2700	100	59	NA	NA	NA	NA
	2700	-100	59	NA	31.0°	NA	0.80
	2700	100	-59	42.2°	NA	0.75	NA
Double-negative	-2700	-100	59	-42.2°	NA	0.66	NA
	-2700	100	-59	NA	-31.0°	NA	0.92
	2700	-100	-59	NA	NA	NA	NA
Triple-negative	-2700	-100	-59	-42.2°	-31.0°	0.23	1.04

where  $|\mathbf{v}_p| = \sqrt{E_M/\rho}$ . It can be easily found that the Poynting vector  $\mathbf{P}$  and the wave vector  $\mathbf{k}$  should be in the opposite directions when the medium possesses both negative P wave modulus and negative mass density. Physically, it means that the direction of the group velocity is opposite to that of the phase velocity in a double-negative elastic medium [26]. Similar discussion can be applied to the S wave propagation.

To study the wave refraction between two elastic media, the P wave incident at the interface ( $y = 0$ ) is considered, as shown in Fig. 1. The material properties of the incident ( $y < 0$ ) and the transmitted ( $y > 0$ ) media are  $(\rho, E_M, \mu)$  and  $(\rho_1, E_{M1}, \mu_1)$ , respectively. The focus will be concentrated on the wave propagations in the transmitted media with double-negative and triple-negative material properties. In the incident medium,  $E_M/\rho > 0$  is required for the incident P wave propagation. As shown in Fig. 1, five unit vectors  $\mathbf{p}_m^n$  representing the directions of elastic wave energy are defined with subscripts  $m = p$  or  $s$  indicating the P or S wave and superscripts  $n = i, r, t$  indicating the incident, reflected or transmitted wave. The P and S waves can be easily distinguished by the red arrows and the green arrows in the figure, respectively. As indicated in Fig. 1, the incident and transmitted wave energies always travel towards the  $+y$  side while the reflected wave energy travels towards the  $-y$  side, which can be expressed as:

$$\begin{aligned}
 \mathbf{p}_p^i &= \sin \alpha \mathbf{e}_x + \cos \alpha \mathbf{e}_y \\
 \mathbf{p}_p^r &= \sin \alpha' \mathbf{e}_x - \cos \alpha' \mathbf{e}_y \\
 \mathbf{p}_s^r &= \sin \beta' \mathbf{e}_x - \cos \beta' \mathbf{e}_y \\
 \mathbf{p}_p^t &= \sin \alpha_1 \mathbf{e}_x + \cos \alpha_1 \mathbf{e}_y \\
 \mathbf{p}_s^t &= \sin \beta_1 \mathbf{e}_x + \cos \beta_1 \mathbf{e}_y
 \end{aligned} \tag{4}$$

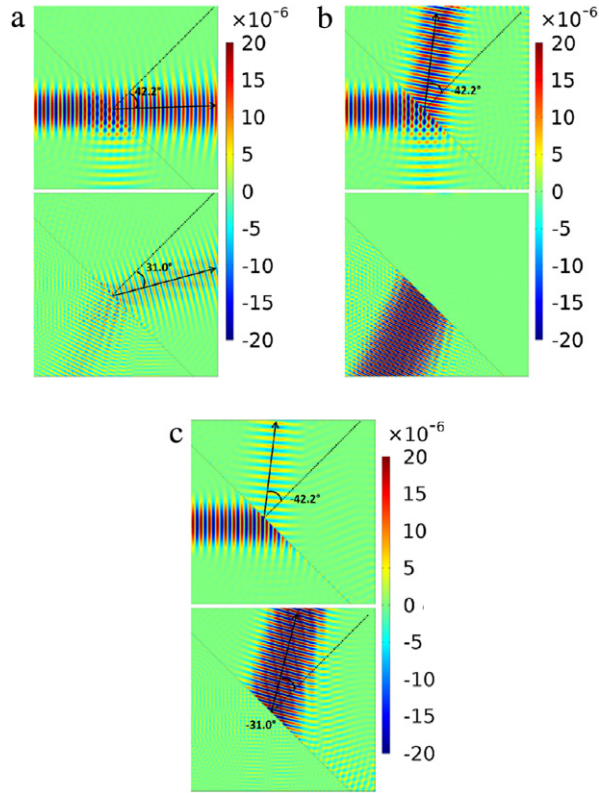


**Fig. 2.** The divergence (top) and curl (bottom) of the simulated wave fields for (a) all-positive transmitted medium, (b) double-negative transmitted medium (negative  $\rho$  and negative  $E_M$ ) and (c) triple-negative transmitted medium. The black dotted line represents the normal direction of the interface and the black solid lines with arrows represent the predictions of the directions of the refracted waves.

where  $\alpha$ ,  $\alpha'$ ,  $\beta'$ ,  $\alpha_1$ ,  $\beta_1$  are denoted as the angles of the incident P wave, the reflected P wave, the reflected S wave, the transmitted P wave and the transmitted S wave, respectively.  $\mathbf{e}_x$  and  $\mathbf{e}_y$  are the unit vectors along  $x$  direction and  $y$  direction, respectively. The range of the angles is restricted to be within  $(-\pi/2, \pi/2)$ . For example, if  $\alpha_1 < 0$  and  $\beta_1 < 0$ , negative refractions of both P wave and S wave occur.

In an isotropic medium, the velocities of the P and S waves can be defined as  $c_p = \sqrt{E_M/\rho}$  and  $c_s = \sqrt{\mu/\rho}$ , respectively. On one side, for an elastic medium with positive mass density, the signs of the P wave modulus and the shear wave modulus will determine whether the P and S waves are forward propagating waves or evanescent waves, respectively. On the other side, for an elastic medium with the negative mass density, only negative P wave modulus and negative shear wave modulus can guarantee the backward propagations of the P and S waves inside the medium, respectively. Here, forward or backward propagating waves in the elastic medium are distinguished based on whether the direction of the wave vector  $\mathbf{k}_m^n$  is the same as, or opposite to, the direction of the unit vector  $\mathbf{p}_m^n$ . Therefore, the propagating wave vectors  $\mathbf{k}_m^n$  can be rewritten in terms of  $\mathbf{p}_m^n$  as:

$$\begin{cases} \mathbf{k}_p^i = \frac{\omega}{c_p} \text{sign}(\rho) \mathbf{p}_p^i \\ \mathbf{k}_p^r = \frac{\omega}{c_p} \text{sign}(\rho) \mathbf{p}_p^r, \quad \text{for } y < 0 \\ \mathbf{k}_s^r = \frac{\omega}{c_s} \text{sign}(\rho) \mathbf{p}_s^r \end{cases} \quad (5a)$$

and

$$\begin{cases} \mathbf{k}_p^t = \frac{\omega}{c_{p1}} \text{sign}(\rho_1) \mathbf{p}_p^t \\ \mathbf{k}_s^t = \frac{\omega}{c_{s1}} \text{sign}(\rho_1) \mathbf{p}_s^t \end{cases}, \quad \text{for } y > 0 \quad (5b)$$

where  $\text{sign}(\epsilon) = \begin{cases} 1, & \text{for } \epsilon > 0 \\ -1, & \text{for } \epsilon < 0 \end{cases}$ . The forward or backward propagating wave can be unambiguously determined by the value ( $\pm 1$ ) of the sign function. For the evanescent waves, since no energy can be transmitted, the sign function would have

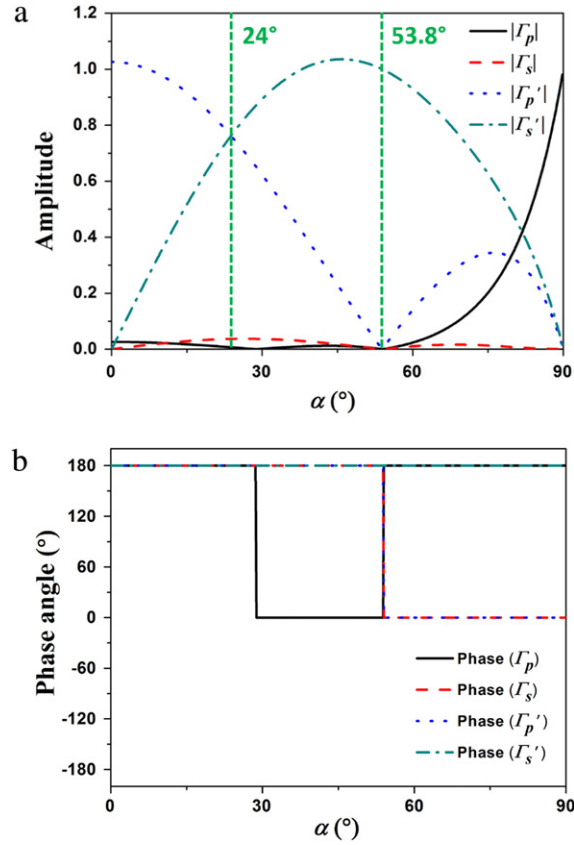


**Fig. 3.** (a) Amplitudes and (b) phase angles of the reflected and refracted P and S waves at different angles of incidence when the transmitted medium has triple-negative material properties.

no meaning and can be retained for a unified formulation. The displacements for the waves, represented by the thin blue arrows in Fig. 1, are then defined as

$$\begin{aligned}
 \mathbf{u}_p^i &= A_i \text{sign}(\rho) \mathbf{p}_p^i \exp(-i\mathbf{k}_p^i \cdot \mathbf{x}) \\
 \mathbf{u}_p^r &= A_r \text{sign}(\rho) \mathbf{p}_p^r \exp(-i\mathbf{k}_p^r \cdot \mathbf{x}) \\
 \mathbf{u}_s^r &= B_r \text{sign}(\rho) (\mathbf{p}_s^r \times \mathbf{e}_z) \exp(-i\mathbf{k}_s^r \cdot \mathbf{x}) \\
 \mathbf{u}_p^t &= A_t \text{sign}(\rho_1) \mathbf{p}_p^t \exp(-i\mathbf{k}_p^t \cdot \mathbf{x}) \\
 \mathbf{u}_s^t &= B_t \text{sign}(\rho_1) (\mathbf{p}_s^t \times \mathbf{e}_z) \exp(-i\mathbf{k}_s^t \cdot \mathbf{x})
 \end{aligned} \tag{6}$$

where  $A_r$ ,  $A_t$ ,  $B_r$  and  $B_t$  are complex amplitudes to be determined from the given incident wave amplitude  $A_i$ .  $\mathbf{e}_z$  is the unit vector along the direction perpendicular to the  $x$ - $y$  plane.

By requiring the displacement continuity condition at the wave incident point ( $\mathbf{x} = 0$ ),  $\mathbf{u}_p^i + \mathbf{u}_p^r + \mathbf{u}_s^r = \mathbf{u}_p^t + \mathbf{u}_s^t$ , a generalized Snell's law can be obtained as:

$$\begin{aligned}
 \text{sign}(\rho) \frac{\sin \alpha}{c_p} &= \text{sign}(\rho) \frac{\sin \alpha'}{c_p} = \text{sign}(\rho) \frac{\sin \beta'}{c_s} = \text{sign}(\rho_1) \frac{\sin \alpha_1}{c_{p1}} \\
 &= \text{sign}(\rho_1) \frac{\sin \beta_1}{c_{s1}}.
 \end{aligned} \tag{7}$$

For incident and transmitted media with all positive material properties, the proposed generalized Snell's law has the same form as that of the conventional Snell's law. For incident medium with positive material properties and transmitted medium with simultaneously negative effective mass density and modulus, negative angles of refraction can be obtained from Eq. (7).

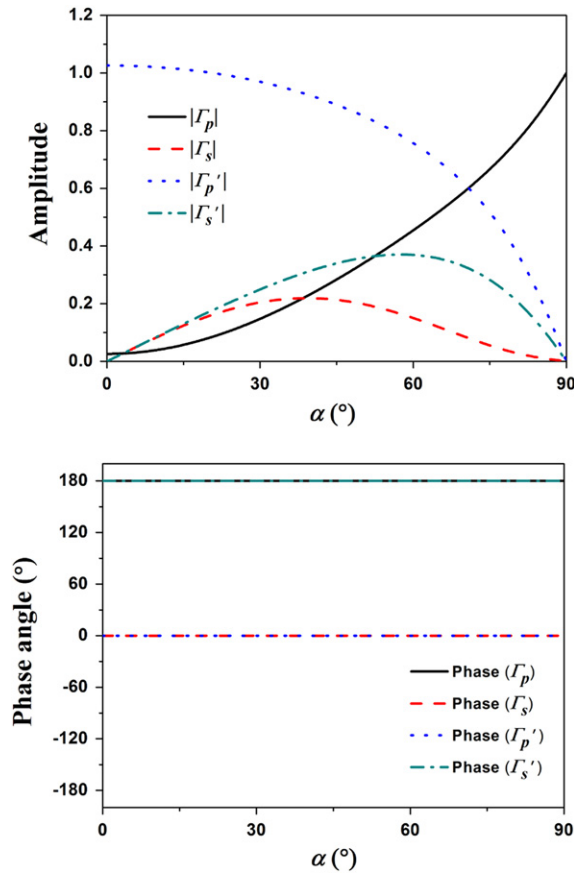


**Fig. 4.** (a) Amplitudes and (b) phase angles of the reflected and refracted P and S waves at different angles of incidence when the transmitted medium has all-positive material properties.

Combining the displacement and stress continuity conditions at the wave incident point will result in:

$$\begin{bmatrix}
 -\sin \alpha & \cos \beta & \text{sign}\left(\frac{\rho_1}{\rho}\right) \sin \alpha_1 & \text{sign}\left(\frac{\rho_1}{\rho}\right) \cos \beta_1 \\
 \cos \alpha & \sin \beta & \text{sign}\left(\frac{\rho_1}{\rho}\right) \cos \alpha_1 & -\text{sign}\left(\frac{\rho_1}{\rho}\right) \sin \beta_1 \\
 -(E_M - \mu + \mu \cos 2\alpha) & -\mu \frac{c_p}{c_s} \sin 2\beta & \frac{c_p}{c_{p1}} (E_{M1} - \mu_1 + \mu_1 \cos 2\alpha_1) & -\mu_1 \frac{c_p}{c_{s1}} \sin 2\beta_1 \\
 \mu \sin 2\alpha & -\mu \frac{c_p}{c_s} \cos 2\beta & \frac{c_p}{c_{p1}} \mu_1 \sin 2\alpha_1 & \mu_1 \frac{c_p}{c_{s1}} \cos 2\beta_1
 \end{bmatrix}
 \begin{bmatrix}
 \Gamma_p \\
 \Gamma_s \\
 \Gamma_p' \\
 \Gamma_s'
 \end{bmatrix}
 =
 \begin{bmatrix}
 \sin \alpha \\
 \cos \alpha \\
 E_M - \mu + \mu \cos 2\alpha \\
 \mu \sin 2\alpha
 \end{bmatrix}
 \tag{8}$$

where  $\begin{cases} \Gamma_p = \frac{A_r}{A_i} \\ \Gamma_s = \frac{B_r}{A_i} \end{cases}$  and  $\begin{cases} \Gamma_p' = \frac{A_t}{A_i} \\ \Gamma_s' = \frac{B_t}{A_i} \end{cases}$  are reflection and transmission coefficients of the P and S waves which can be determined by solving the linear equations above.

### 3. Numerical results

In this section, we will demonstrate anomalous wave propagation and reflection from the semi-infinite elastic medium with all positive material properties to the semi-infinite elastic media with different combinations of negative material

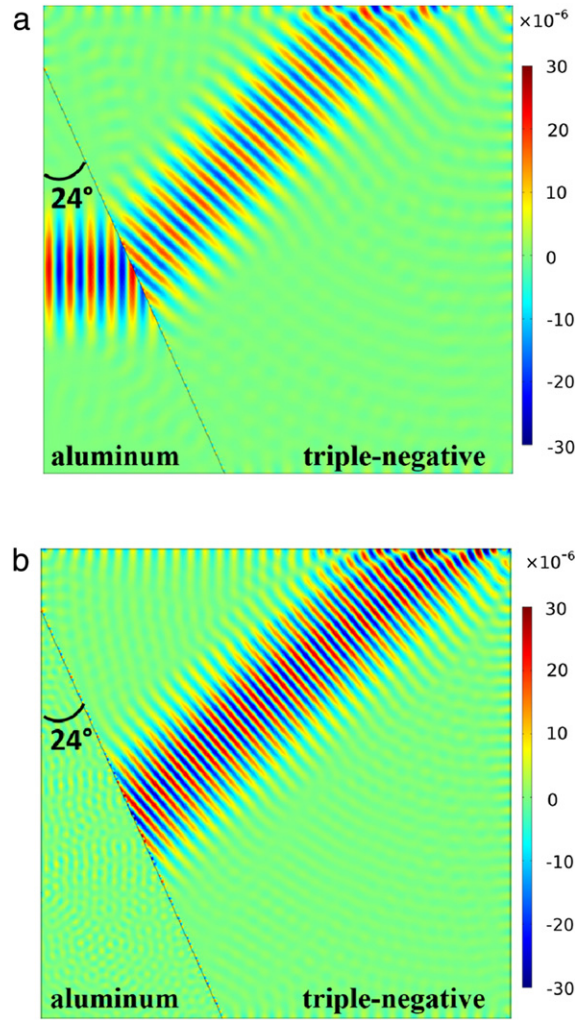


**Fig. 5.** (a) The divergence and (b) curl of the simulated wave fields at angle of incidence  $\alpha = 24^\circ$  for transmitted medium with triple-negative material properties.

properties by using the derived generalized Snell's law and the calculated reflection and transmission coefficients for both P and S waves. The effects of fixed and changing angles of incidence are discussed in Sections 3.1 and 3.2, respectively.

### 3.1. Wave propagation and reflection from positive medium to negative medium with fixed angle of incidence

In this subsection, we study the P wave incidence at a fixed angle,  $\alpha = 45^\circ$ . Without loss of generality, the incident medium is selected as aluminum with  $\rho = 2700 \text{ kg/m}^3$ ,  $E_M = 111 \text{ GPa}$  and  $\mu = 26 \text{ GPa}$ . Eight different transmitted media are considered and cataloged into 4 classes: all-positive, single-negative, double-negative and triple-negative. Their material properties are listed in Table 1. In the table, the angles of the refracted P and S waves,  $\alpha_1$  and  $\beta_1$ , are predicted by using the generalized Snell's law in Eq. (7). The amplitudes of the transmission coefficients of the refracted P and S waves,  $|T_p'|$  and  $|T_s'|$ , are calculated by solving Eq. (8).

In order to verify the analytical predictions of the refraction angles, full-scale wave simulations using the commercial finite element (FE) software COMSOL are performed. In the numerical simulations, a  $45^\circ$  triangular prism (L: 500 mm  $\times$  W: 500 mm) made of aluminum is bonded to the transmitted media with all-positive, double-negative and triple-negative material properties. A Gaussian beam of the P wave with operating frequency 250 kHz is launched horizontally from the left side of the wedge. In the simulations, perfect matched layers (PMLs) are applied to the boundaries of the media in order to avoid any boundary reflections. Both the refracted P wave and the refracted S wave could be generated at the interface between the two elastic media. To separate the P and S wave modes in the near field, the divergence and curl of the wave displacement fields are numerically calculated to represent the pure P wave field and the pure S wave field, respectively [27]. Fig. 2(a)–(c) demonstrates the simulation results for all-positive, double-negative and triple-negative transmitted media, respectively.

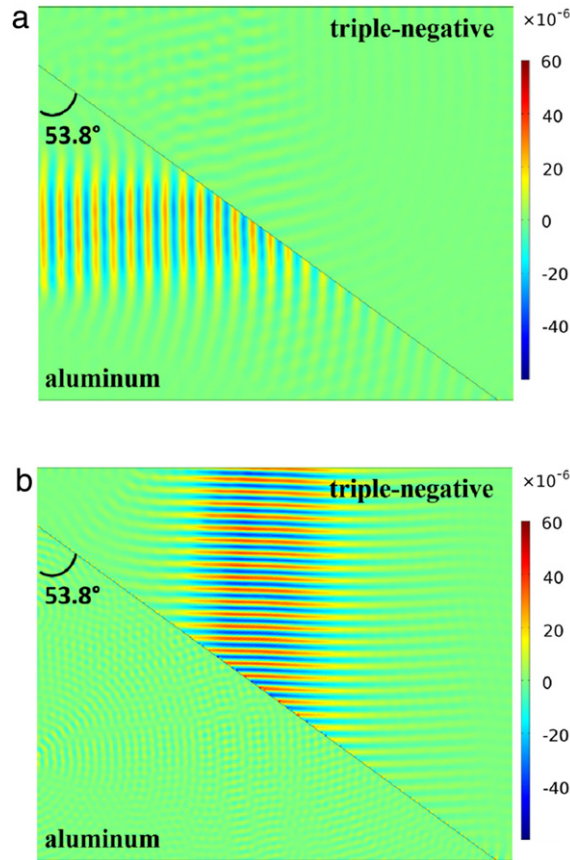


**Fig. 6.** (a) The divergence and (b) curl of the simulated wave fields at angle of incidence  $\alpha = 53.8^\circ$  for transmitted medium with triple-negative material properties.

By applying 2D spatial Fourier transform [28] to the refracted wave fields, one can easily determine the angles of refraction which are found to be in good agreement with the analytical predictions (black solid lines with arrows in the figure) from the proposed generalized Snell's law. Furthermore, it is found that the refracted P wave has much stronger amplitude than that of the refracted S wave in the all-positive transmitted medium, as shown in Fig. 2(a). The result is confirmed by comparing the amplitudes of the corresponding transmission coefficients in Table 1. In contrast to the case of all-positive transmitted medium, it is noticed that the negatively refracted P wave is much weaker in amplitude than the negatively refracted S wave in triple-negative transmitted medium, as shown in Fig. 2(c). In Fig. 2(b), only the negatively refracted P wave can be observed and the refracted S wave is an evanescent wave in the double-negative transmitted medium due to the opposite signs of the mass density and the shear wave modulus.

### 3.2. Wave propagation and reflection from positive medium to negative medium with changing angles of incidence

In this subsection, quantitative analysis on the reflected and refracted P and S waves and the effect of different angles of incidence are discussed for both double-negative and triple-negative transmitted media. The wave reflection and transmission coefficients as functions of the angle of incidence will be investigated to demonstrate some unusual wave propagation phenomena. It is worth mentioning that the analysis on the wave propagation from negative medium to standard positive medium can be easily performed based on the proposed theoretical framework.

#### 3.2.1. The effect of changing angles of incidence on the triple-negative transmitted medium

First, the wave reflection and transmission coefficients as functions of the angle of incidence will be studied for transmitted medium with triple-negative material properties which are listed in Table 1. The incident medium is aluminum. For the angle of incidence changing from  $\alpha = 0^\circ$  to  $\alpha = 90^\circ$ , Fig. 3(a) and (b) shows the amplitudes and the phase angles of the reflection and transmission coefficients of the P and S waves, respectively. For comparison purposes, the corresponding results of the all-positive transmitted medium are also demonstrated in Fig. 4.

From Fig. 3(a), it can be found that the amplitudes of the refracted P and S waves have the same value when  $\alpha = 24^\circ$ , which is confirmed by the full-scale wave simulations in Fig. 5. When the angle of incidence goes beyond  $24^\circ$ , the amplitude

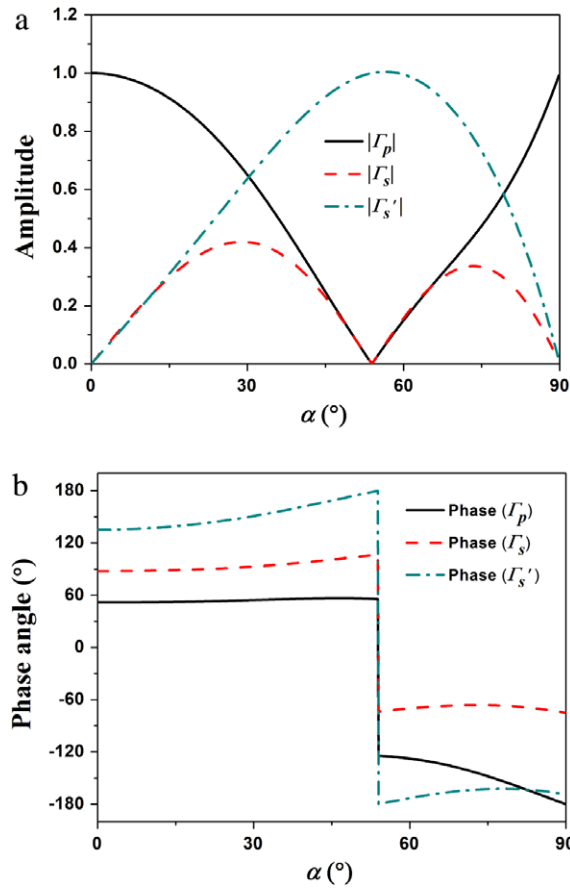


**Fig. 7.** (a) Amplitudes and (b) phase angles of the reflected P and S waves and the refracted S wave at different angles of incidence when the transmitted medium has negative mass density and negative shear wave modulus.

of the refracted S wave in the triple-negative transmitted medium becomes larger than that of the refracted P wave, which is different from the results in Fig. 4(a) where the refracted P wave always dominates in the all-positive transmitted medium. Also, it is noticed that the refracted waves (both P and S) in the triple-negative transmitted medium have much larger amplitudes than those of the reflected waves. Furthermore, a very interesting phenomenon can be observed in Fig. 3(a) when the angle of incidence reaches  $\alpha = 53.8^\circ$ . At  $\alpha = 53.8^\circ$ , the amplitudes of the reflected P, reflected S and refracted P waves are all zero but the amplitude of the refracted S wave is equal to that of the incident P wave. Therefore, the incident P wave is completely converted to the refracted S wave in the transmitted medium with triple-negative material properties. The complete wave mode conversion is a unique property of elastic metamaterials with negative material properties [12]. The similar shear polarization of elastic waves can also be achieved in a system with structured interface [29] where the refracted shear wave dominates in the transmitted medium but non-zero reflected waves still exist in the incident medium. In order to confirm the occurrence of the complete wave mode conversion, full-scale wave simulation is conducted at  $\alpha = 53.8^\circ$  for the transmitted medium with triple-negative material properties which are listed in Table 1. Examining the divergence and curl of the simulated wave displacement fields, as shown in Fig. 6(a) and (b) respectively, we can find neither wave reflections nor P wave refraction. Therefore, it is evident that the incident P wave is completely converted to the refracted S wave. The angle between the incident and refracted waves is  $90^\circ$  in the negative refraction region. Finally, changes in the phase angles of the transmission and reflection coefficients at different angles of incidence are observed in Fig. 3(b) for triple-negative transmitted medium, while constant phase angles are observed in Fig. 4(b) for all-positive transmitted medium.

### 3.2.2. The effect of changing angles of incidence on the double-negative transmitted medium

In this subsection, the wave reflection and transmission coefficients as functions of the angle of incidence will be studied for transmitted medium with double-negative material properties. As shown in Table 1, the double-negative transmitted medium can have one of the three different combinations of material properties. However, only the two combinations with negative mass density can generate refracted P or S wave. First, let us study the case of the transmitted medium with negative mass density and negative shear wave modulus. Fig. 7(a) and (b) shows the amplitudes and the phase angles of the coefficients of the P and S waves, respectively. Since the mass density and the P-wave modulus of the transmitted medium

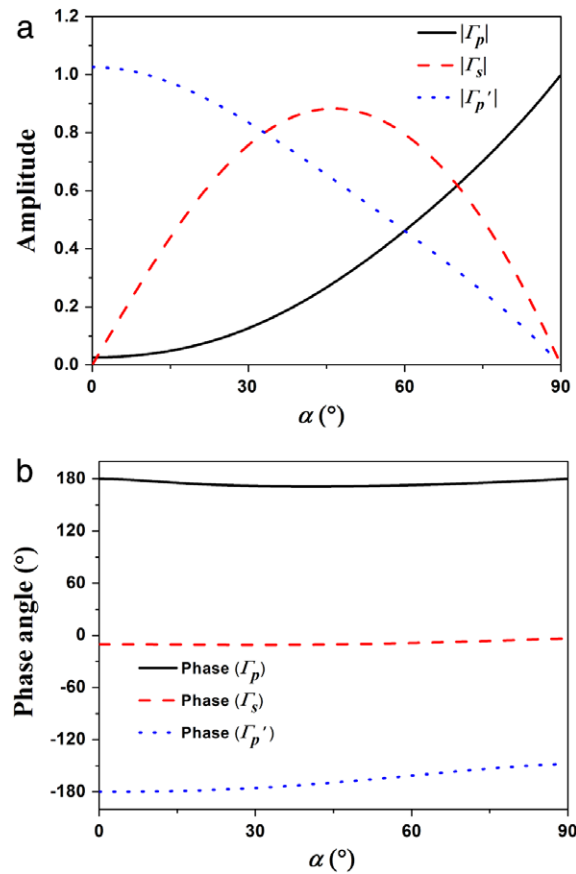


**Fig. 8.** (a) Amplitudes and (b) phase angles of the reflected P and S waves and the refracted P wave at different angles of incidence when the transmitted medium has negative mass density and negative P-wave modulus.

have different signs, the refracted P wave has imaginary velocity and therefore, is evanescent wave which is not plotted in Fig. 7. It can be found that the complete wave mode conversion occurs at  $\alpha = 53.8^\circ$ , which is the same phenomenon that we have observed in the case of the triple-negative transmitted medium. Unlike the case of the triple-negative transmitted medium in Fig. 3(a), the reflected P and S waves are found to have much larger amplitudes at other angles of incidence, as shown in Fig. 7(a). Fig. 7(b) shows that the phase angles of the reflected and refracted waves jump from positive values to negative values once the angle of incidence reaches to  $\alpha = 53.8^\circ$ , while no negative phase angles can be found in the case of the triple-negative transmitted medium, as shown in Fig. 3(b).

Second, we study the case of the transmitted medium with negative mass density and negative P-wave modulus. Since the refracted S wave is an evanescent wave, no components of the refracted S wave are plotted in Fig. 8. The amplitudes and the phase angles of the reflected P and S waves and the refracted P wave are shown in Fig. 8(a) and (b), respectively. Comparing with Fig. 7, no zero-reflection can be found at any angle of incidence in Fig. 8(a) and no dramatic jump in the phase angles can be found in Fig. 8(b) either.

#### 4. Conclusions

In this paper, plane wave propagation and reflection in the semi-infinite elastic media with doubly or triply negative material properties are studied analytically and numerically. The unique negative refractions for both P and S waves are studied by the proposed generalized Snell's law. Quantitative characterization of the effects of different combinations of negative material properties on the anomalous wave propagation is investigated for various angles of incidence. The study can serve as the theoretical foundation for engineering and designing general metamaterial-based elastic wave devices.

#### Acknowledgment

This work was supported by Air Force Office of Scientific Research under Grant No. AF 9550-15-1-0061 with Program Manager Dr. Byung-Lip (Les) Lee.

## References

- [1] V.G. Veselago, The electrodynamics of substances with simultaneously negative values of  $\epsilon$  and  $\mu$ , *Sov. Phys. Usp.* 10 (1968) 509.
- [2] R.A. Shelby, D.R. Smith, S. Schultz, Experimental verification of a negative index of refraction, *Science* 292 (2001) 77–79.
- [3] S. Zhang, L.L. Yin, N. Fang, Focusing ultrasound with an acoustic metamaterial network, *Phys. Rev. Lett.* 102 (2009) 194301.
- [4] Z. Liu, X. Zhang, Y. Mao, Y.Y. Zhu, Z. Yang, C.T. Chan, P. Sheng, Locally resonant sonic materials, *Science* 289 (2000) 1734–1736.
- [5] N. Fang, D. Xi, J. Xu, M. Ambati, W. Srituravanich, C. Sun, X. Zhang, Ultrasonic metamaterials with negative modulus, *Nature Mater.* 5 (2006) 452–456.
- [6] G.W. Milton, J.R. Willis, On modifications of Newton's second law and linear continuum elastodynamics, *Proc. Roy. Soc. A* 463 (2007) 855–880.
- [7] A.B. Movchan, L.I. Slepyan, Band gap Green's functions and localized oscillations, *Proc. Roy. Soc. A* 463 (2007) 2709–2727.
- [8] R. Zhu, G.L. Huang, H.H. Huang, C.T. Sun, Experimental and numerical study of guided wave propagation in a thin metamaterial plate, *Phys. Lett. A* 375 (2011) 2863–2867.
- [9] X.M. Zhou, G.K. Hu, Analytic model of elastic metamaterials with local resonances, *Phys. Rev. B* 79 (2009) 195109.
- [10] X.N. Liu, G.K. Hu, G.L. Huang, C.T. Sun, An elastic metamaterial with simultaneously negative mass density and bulk modulus, *Appl. Phys. Lett.* 98 (2011) 251907.
- [11] R. Zhu, X.N. Liu, G.K. Hu, C.T. Sun, G.L. Huang, Negative refraction of elastic waves at the deep subwavelength scale in a single-phase metamaterial, *Nature Commun.* 5 (2014) 5510.
- [12] Y. Wu, Y. Lai, Z.Q. Zhang, Elastic metamaterials with simultaneously negative effective shear modulus and mass density, *Phys. Rev. Lett.* 107 (2011) 105506.
- [13] M. Brun, S. Guenneau, A.B. Movchan, D. Bigoni, Dynamics of structural interfaces: filtering and focusing effects for elastic waves, *J. Mech. Phys. Solids* 58 (2010) 1212–1224.
- [14] T. Antonakakis, R.V. Craster, S. Guenneau, Homogenisation of elastic photonic crystals and dynamic anisotropy, *J. Mech. Phys. Solids* 71 (2014) 84–96.
- [15] S. Brûlé, E.H. Javelaud, S. Enoch, S. Guenneau, Experiments on seismic metamaterials: molding surface waves, *Phys. Rev. Lett.* 112 (2014) 133901.
- [16] R. Zhu, X.N. Liu, G.K. Hu, C.T. Sun, G.L. Huang, A chiral elastic metamaterial beam for broadband vibration suppression, *J. Sound Vib.* 333 (2014) 2759–2773.
- [17] J.S. Chen, B. Sharma, C.T. Sun, Dynamic behavior of sandwich structure containing spring-mass resonators, *Compos. Struct.* 93 (2011) 2120–2125.
- [18] X. Yan, R. Zhu, G.L. Huang, F.G. Yuan, Focusing guided waves using surface bonded elastic metamaterials, *Appl. Phys. Lett.* 103 (2013) 121901.
- [19] R. Zhu, X.N. Liu, G.L. Huang, H.H. Huang, C.T. Sun, Microstructural design and experimental validation of elastic metamaterial plates with anisotropic mass density, *Phys. Rev. B* 86 (2012) 144307.
- [20] D. Bigoni, S. Guenneau, A.B. Movchan, M. Brun, Elastic metamaterials with inertial locally resonant structures: application to lensing and localization, *Phys. Rev. B* 87 (2013) 174303.
- [21] Z.S. Chen, B. Guo, Y.M. Yang, C.C. Cheng, Metamaterials-based enhanced energy harvesting: a review, *Phys. B: Condens. Matter* 438 (2014) 1–8.
- [22] K. Graff, *Wave Motion in Elastic Solids*, Clarendon Press, Oxford, 1975.
- [23] J. Achenbach, *Wave Propagation in Elastic Solids*, Elsevier, Amsterdam, 1975.
- [24] J.M. Carcione, S. Picotti, P-wave seismic attenuation by slow-wave diffusion: effects of inhomogeneous rock properties, *Geophysics* 71 (2006) O1–O8.
- [25] B.A. Auld, *Acoustic Fields and Waves in Solids*, Krieger Publishing Company, Malabar, FL, 1973.
- [26] J. Li, C.T. Chan, Double-negative acoustic metamaterial, *Phys. Rev. E* 70 (2004) 055602.
- [27] Z. Chang, J. Hu, G.K. Hu, R. Tao, Y. Wang, Controlling elastic waves with isotropic materials, *Appl. Phys. Lett.* 98 (2011) 121904.
- [28] M. Ruzzene, Frequency–wavenumber domain filtering for improved damage visualization, *Smart Mater. Struct.* 16 (2007) 2116–2129.
- [29] M. Brun, A.B. Movchan, N.V. Movchan, Shear polarisation of elastic waves by a structured interface, *Contin. Mech. Thermodyn.* 22 (2010) 663–677.